

---

*A global study of 2D dissipative  
diffeomorphisms with a Poincaré homoclinic  
figure-eight.*

*DDAYS 2012, Benicàssim,*

*October 24–26, 2012*

A. Vieiro

(Univ. Barcelona)

Joint work with S. Gonchenko (Univ. Nizhny Nóvgorod) and C. Simó (Univ. Barcelona)

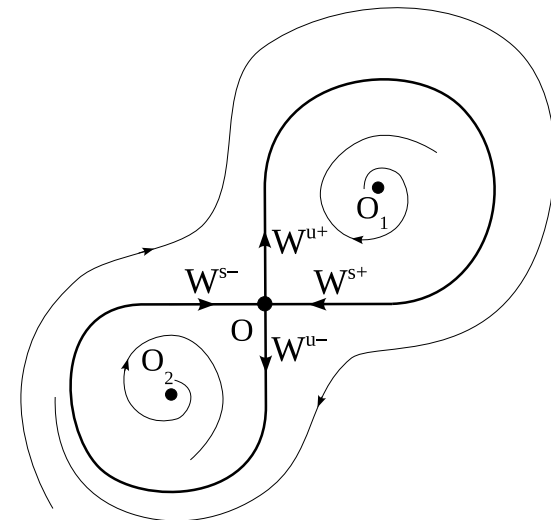
# Introduction

We consider a family  $T_{\mu,\epsilon}$ ,  $\mu \in \mathbb{R}^2$ ,  $\epsilon \in \mathbb{R}$ , of 2D analytic diffeomorphisms.

$T_{\mu,\epsilon}$  can be seen as the **Poincaré map** of a **non-autonomous** ( $2\pi$ -periodic in time)  $\mathcal{O}(\epsilon)$ -perturbation of an **autonomous** family of vector fields  $f_\mu$ .

- The **non-autonomous perturbation** is assumed to be **fixed** and sufficiently **small** (equivalently,  $\epsilon$  is a small given value).
- The family of autonomous systems  $f_\mu$  is a **2-parameter unfolding** of the system  $f_0$ , which we assume to possess a **homoclinic figure-eight** to a **dissipative** saddle point.

Let  $\Gamma^+ = W^{u+} = W^{s+}$  and  $\Gamma^- = W^{u-} = W^{s-}$  be the homoclinic loops of the flow  $f_0$ . Then  $\Gamma_0 = \Gamma^+ \cup \Gamma^-$  is the (unperturbed) homoclinic figure-eight of the saddle  $O$ .

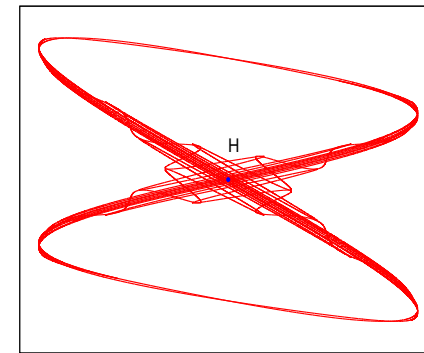
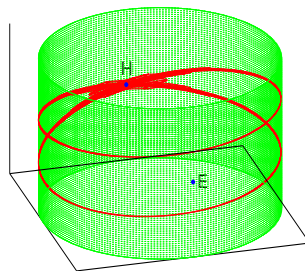
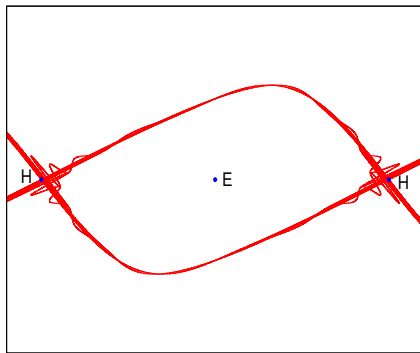


# Motivation

$T_{\mu,\epsilon}$  are **pendulum-like systems** under **forcing and dissipation**.

- **Forcing**  $\Rightarrow$  elliptic point becomes a repellor.
- **Dissipation**  $\Rightarrow$  the dynamics is towards the separatrix.

The **cylinder-sphere-stereo projection** identifies with a **dissipative figure-eight**.



**Device?** pendulum + dissipation proportional to velocity (asymmetric if different bulk left/right shapes) + magnetic field kicks at the minimum to make the fixed points unstable.

# Idea of this talk

---

We want to study the **parameter space** of  $T_{\mu,\epsilon}$  for  $\epsilon$  small fixed. Concretely, we consider:

1. A **qualitative** approach to the full bifurcation diagram.
  - Different dynamics and regions.
  - Homoclinic dynamics. Lobe dynamics.
  - MS & SA boundaries.
2. A **quantitative** approach to the full bifurcation diagram.

We use a **separatrix map model**.

  - Size of the main regions having different dynamics.
  - Scaling properties of the bifurcation diagram.
  - Stability regions related to cubic tangencies.

---

This talk is based on (some of) the results that can be found in

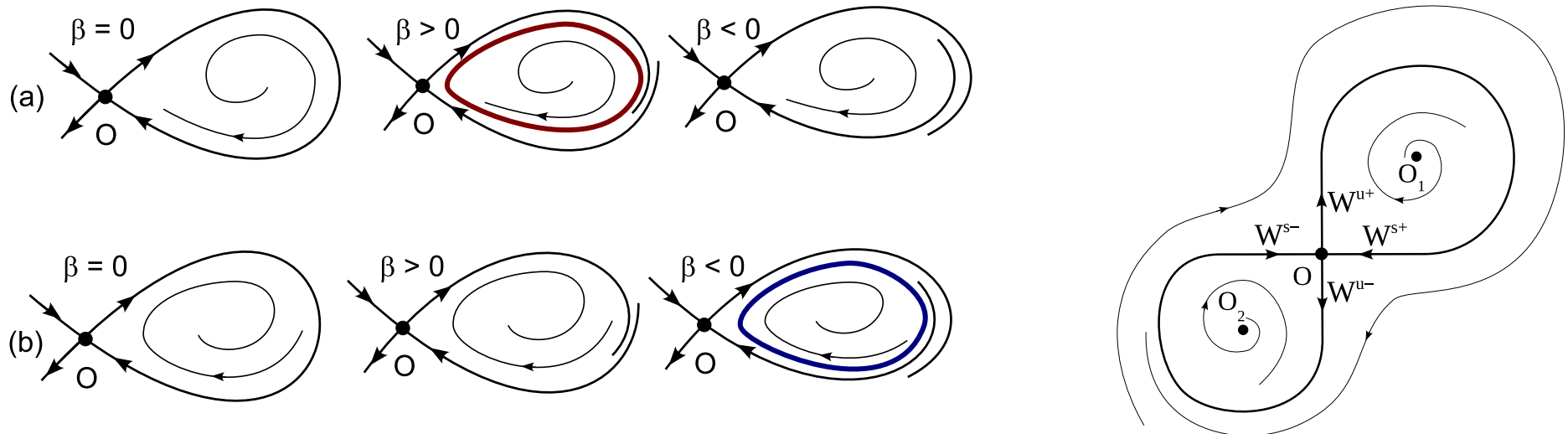
*Richness of dynamics and global bifurcations in systems with a homoclinic figure-eight.*

S.V. Gonchenko , C. Simó and AV, submitted to Nonlinearity.

# The flow (autonomous) case

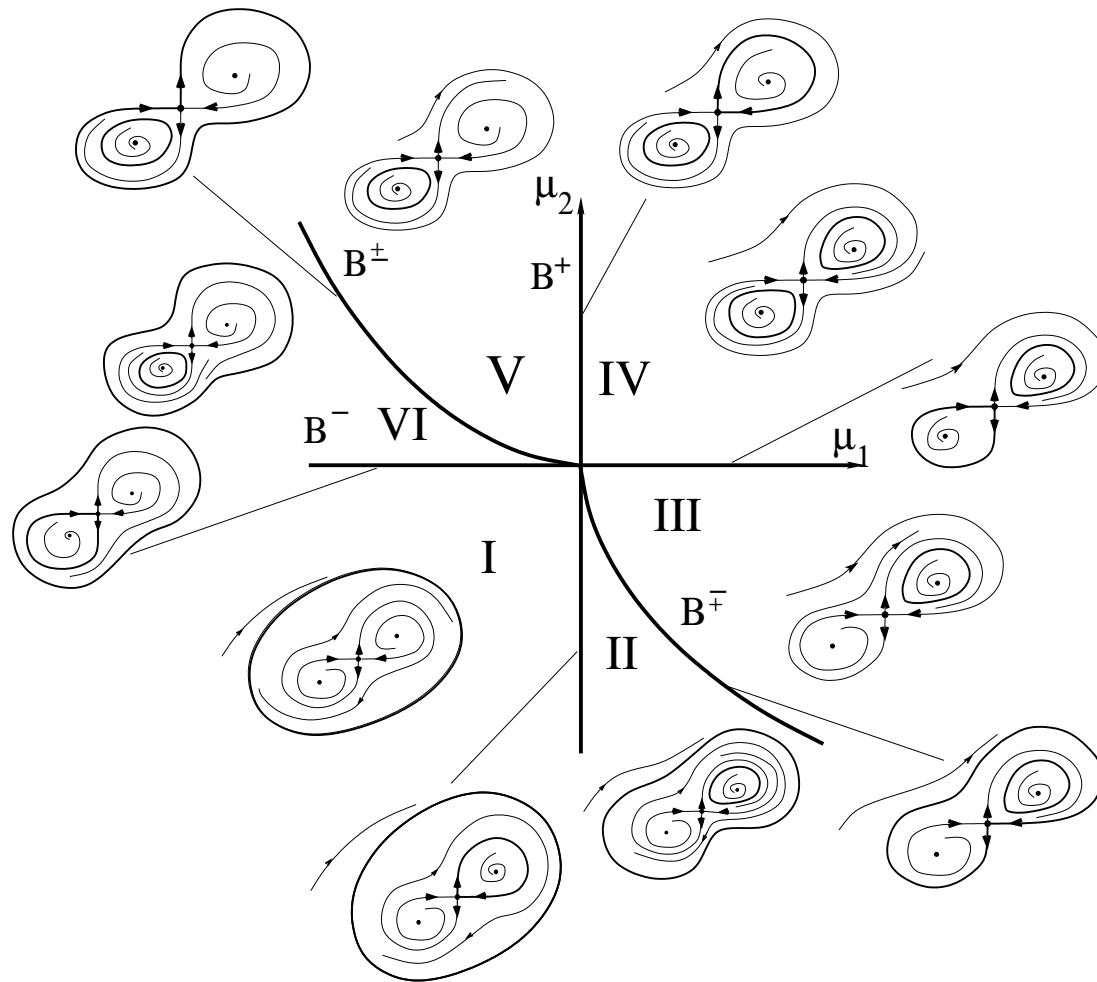
Bifurcations of limit cycles from a homoclinic loop to a saddle:

- Let  $\lambda > 0$  and  $-\gamma < 0$  the characteristic roots of the saddle.
- If  $\sigma = \lambda - \gamma \neq 0$  exactly one limit cycle is born (Andronov-Leontovich).



Left: unfolding a dissipative loop. Right: figure-eight before unfolding.

# The flow case: bifurcation diagram



- **Six regions.**

- **Boundaries:**

$$W^{u+} = W^{s+} \text{ (I} \rightarrow \text{II);}$$

$$W^{u-} = W^{s+} \text{ (II} \rightarrow \text{III);}$$

$$W^{u-} = W^{s-} \text{ (III} \rightarrow \text{IV);}$$

$$W^{u+} = W^{s+} \text{ (IV} \rightarrow \text{V);}$$

$$W^{u+} = W^{s-} \text{ (V} \rightarrow \text{VI);}$$

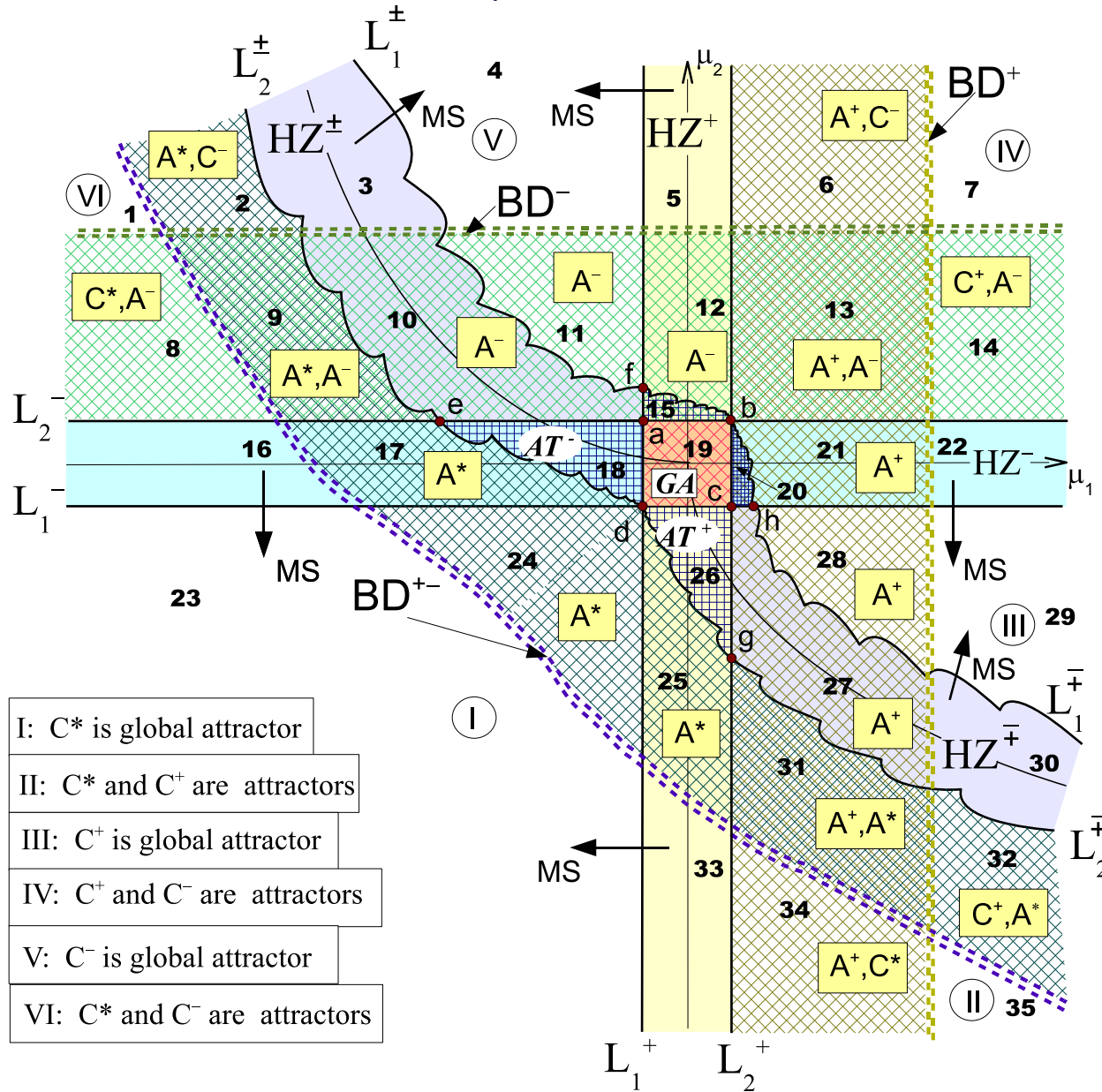
$$W^{u-} = W^{s-} \text{ (VI} \rightarrow \text{I);}$$

D. Turaev. On a case of bifurcation of a contour composed by two homoclinic curves of a saddle.

Methods of the qualitative theory of differential equations, Ed. Gorki, 1984, 162–175.

# The diffeomorphism case: bifurcation diagram

We consider the effect of the non-autonomous perturbation and we look at the Poincaré map.



# Properties of the bifurcation diagram of $T_{\mu,\epsilon}$

1. There appear **35 regions** with different dynamics!
2. These regions are separated by **first/last tangency curves**

$$L_1^+, L_2^+, L_1^-, L_2^-, L_1^\pm, L_2^\pm, L_1^\mp, L_2^\mp,$$

and/or by “curves” that indicate **transitions from “simple” dynamics to strange attractor** (e.g. folding of an invariant curve can cause collision between tangent/normal bundles and create a SA)

$$BD^+, BD^-, BD^{+-}.$$

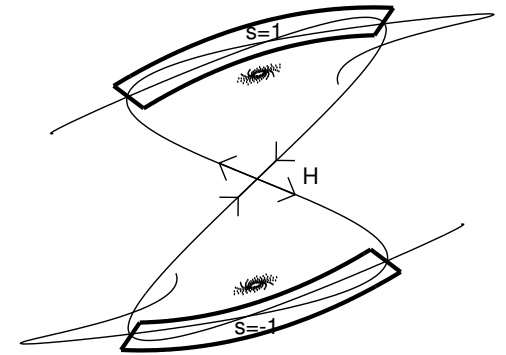
3. Only the  $L_{1,2}^{+,-}$  are **smooth**. The curves  $L_{1,2}^{\pm,\mp}$  have a complicated structure (later) with **infinitely many intervals of smoothness**.
4. Multiple attractors can **coexist**.

→ For a detailed analysis we introduce the following return map model...



# A quantitative model: dissipative separatrix map

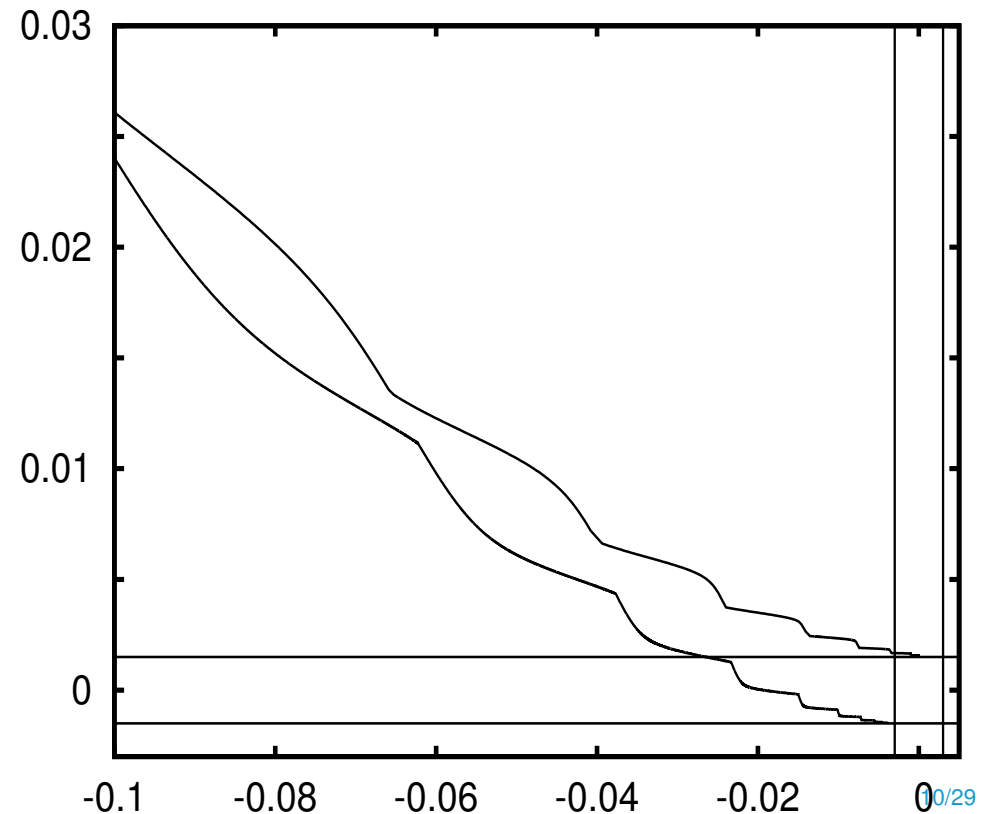
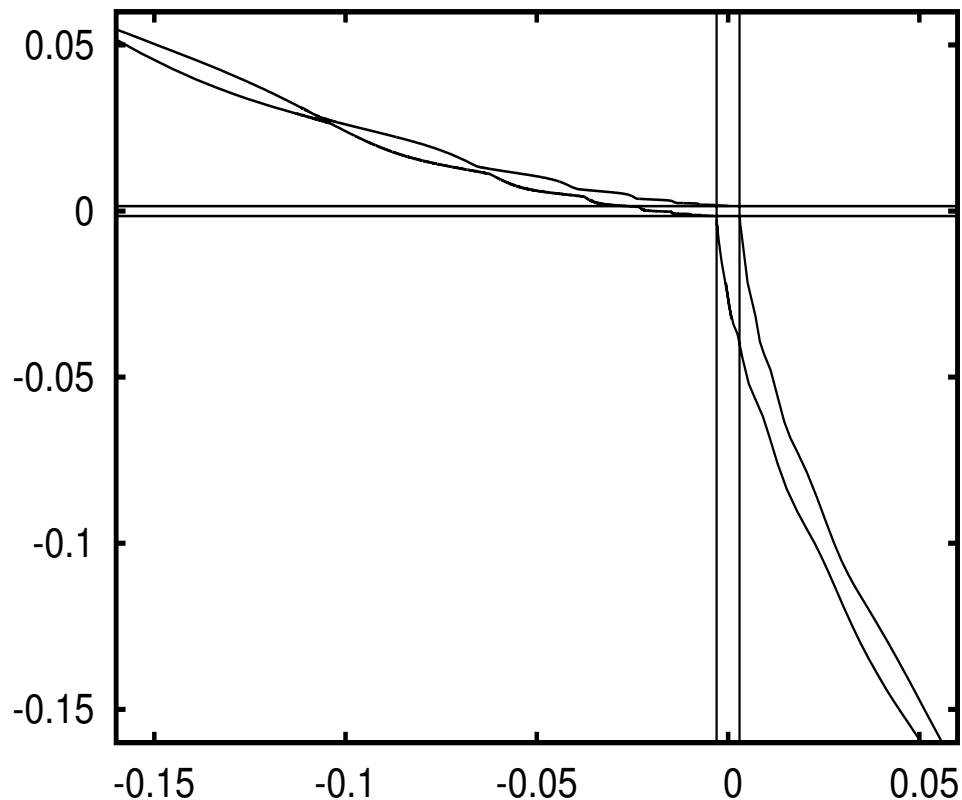
$$M_{a,b,\psi,A,\omega} : \begin{pmatrix} z \\ \eta \\ s \end{pmatrix} \mapsto \begin{pmatrix} z + \omega_j + A \log(|y|) \\ \text{sign}(y)|y|^\psi \\ \text{sign}(y)s \end{pmatrix}$$



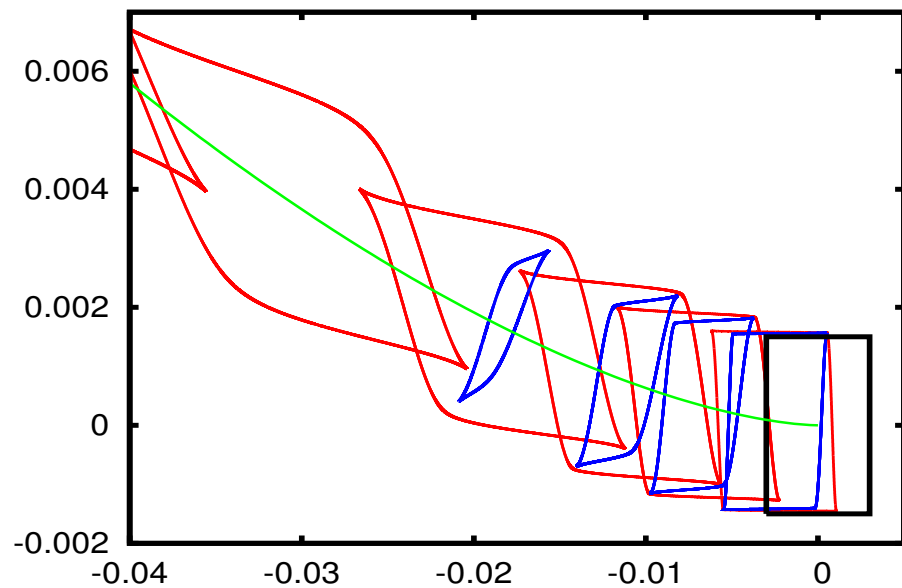
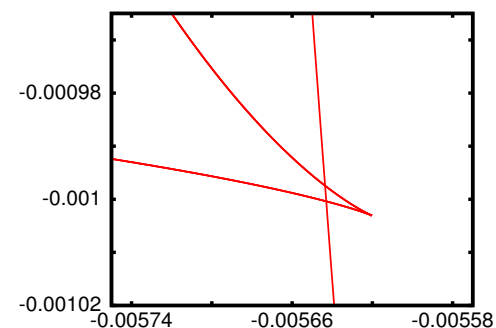
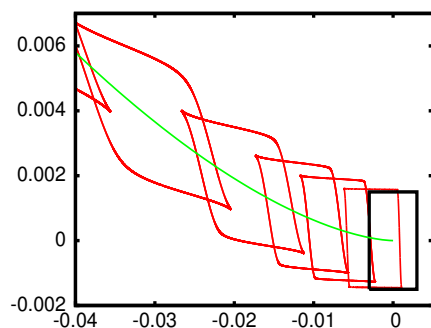
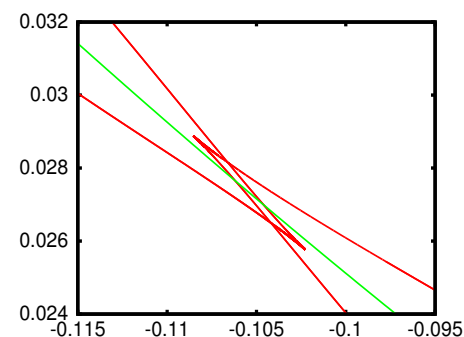
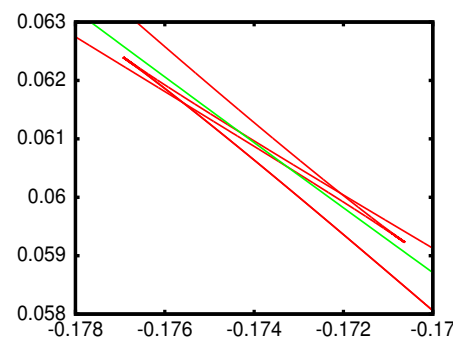
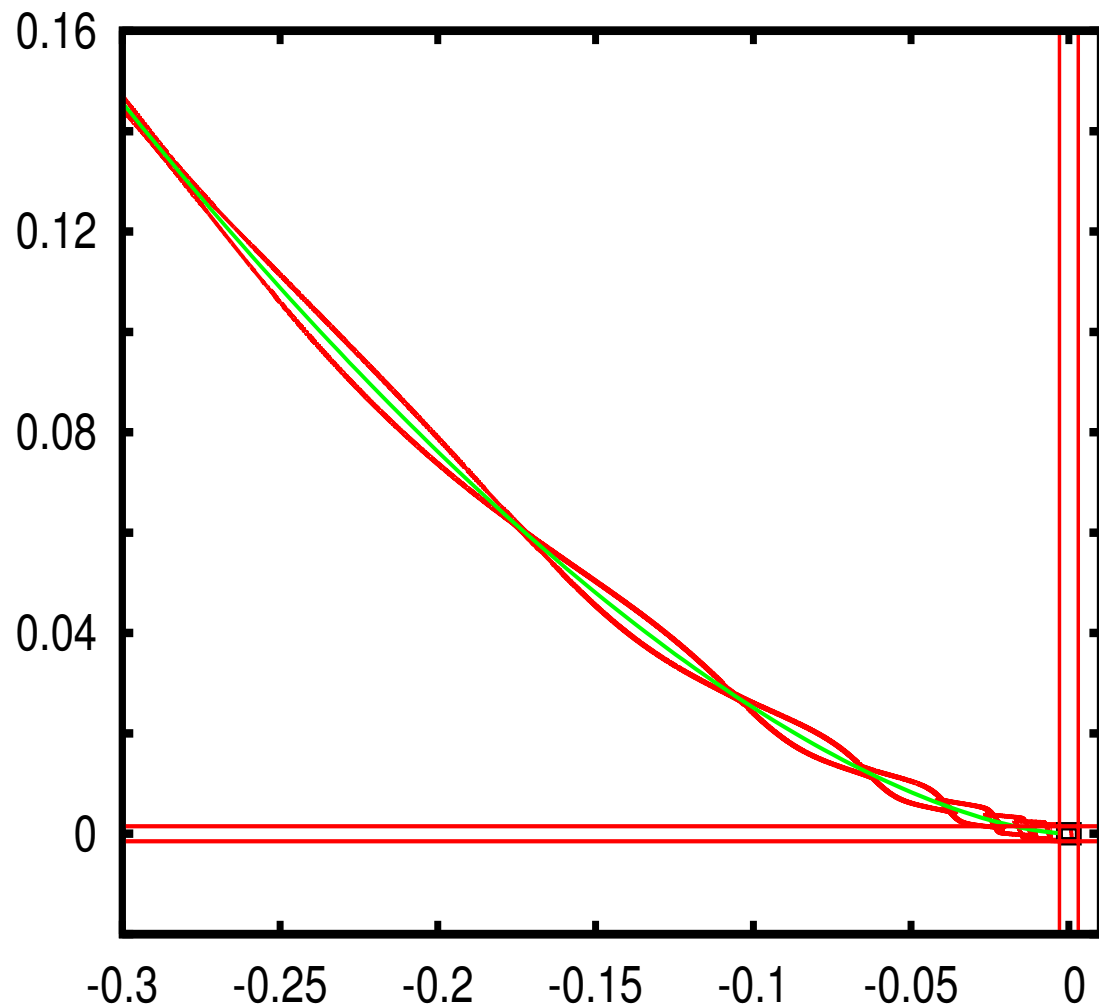
- **FD = two annuli**: the index  $j$  equals 1 if  $s = 1$  and  $j = 2$  if  $s = -1$ .
- $\psi = \lambda/\gamma$  accounts for the dissipation in the passage near the saddle.
- **Returning time** = constant  $\omega_j$  + “flying” time  $A \log(y)$  near the saddle.
- $y = a_j + \eta + b_j \sin(2\pi z)$ , and for both  $\eta$  (distance w.r.t.  $W^u$ ) and  $y$  (distance w.r.t.  $W^s$ ) the positive orientation points towards the saddle.
- If  $a_j = b_j = 0$  both branches  $W^{u/s}$  coincide.  
 For  $b_j = 0$  it mimics the vector field provided  $|a_j| < (\psi - 1)/\psi^{\psi/(\psi-1)}$ .  
 Then  $b_j$  play the role of  $\epsilon$  (they undulate the inv. manifolds).
- In the **simulations**:  $\omega_j = 0$ ,  $A = 2$ ,  $\psi = 1.6$ ,  $b_1 = 0.003$ ,  $b_2 = 0.0015$ .  
 Then  $a_1, a_2$  are taken as **leading parameters** ranging in  $[-0.15, 0.15]$ .

# A preliminary numerical exploration of the model

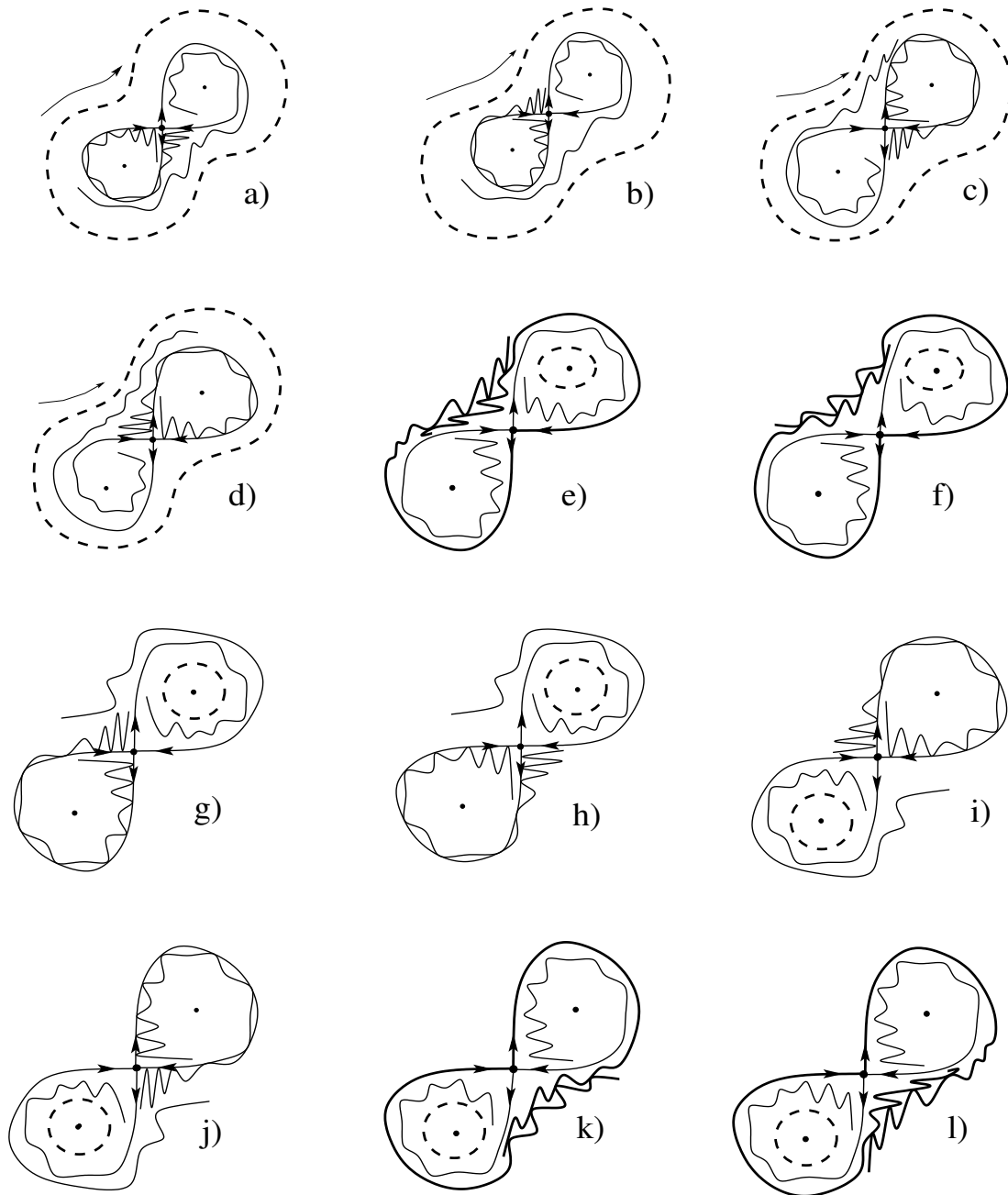
In the  $(a_1, a_2)$ -parameter space we compute **first/last primary homoclinic quadratic tangency curves** between  $W^{u\pm} = \{\eta = 0, s = \pm 1\}$  and  $W^{s\pm} = \{y = 0, s = \pm 1\}$ . The curves  $L_{1,2}^{\pm}$  and  $L_{1,2}^{\mp}$  are the **envelope** of different bifurcating curves (related to different primary quadratic tangencies) that bound a “diagonal” strip with “stair-type” structure. Essentially **8 curves**.



# Bifurcating curves within $HZ^\pm$



# Homoclinic tangencies – phase space



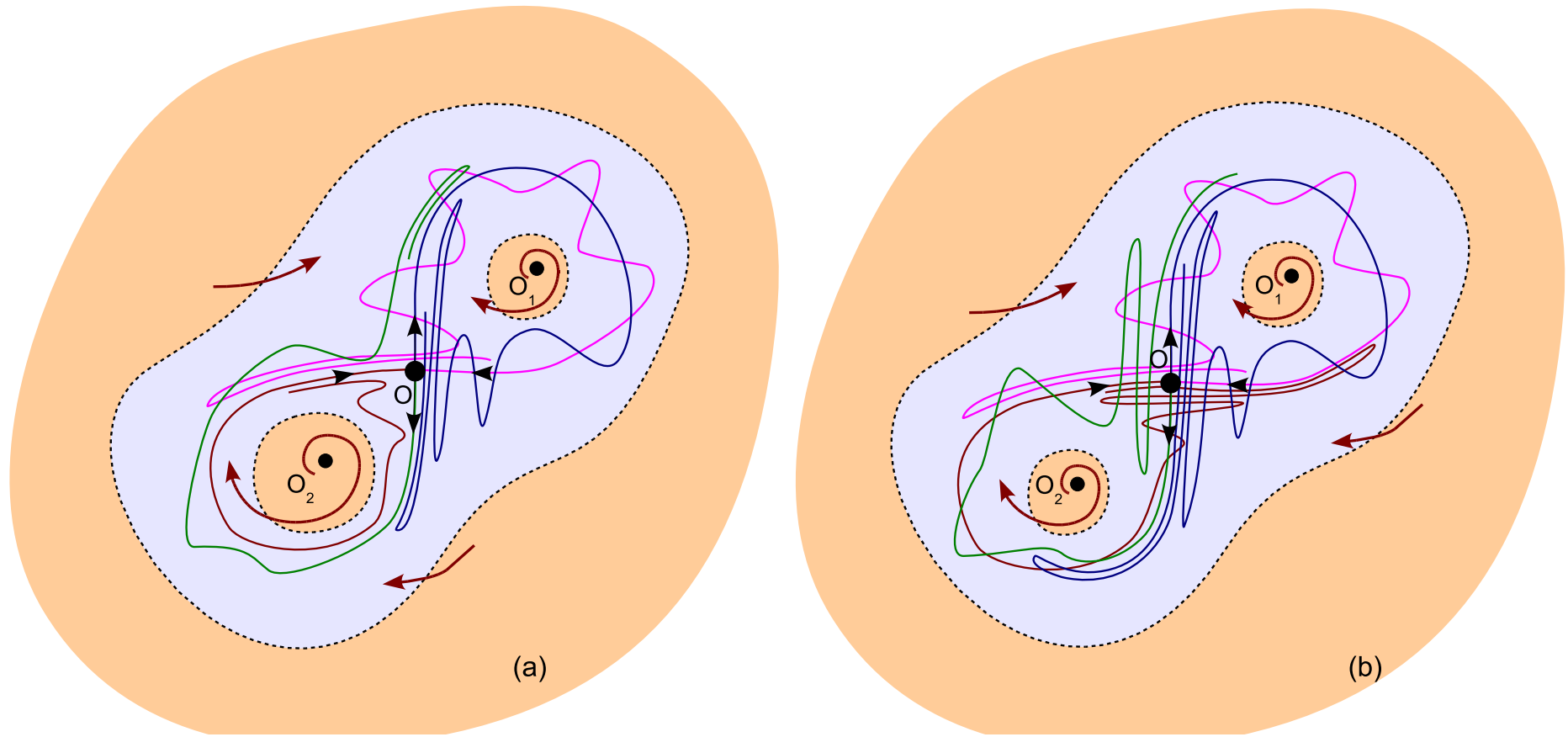
- a)  $\mu \in L_2^-, \mu_1 < 0;$
- b)  $\mu \in L_1^-, \mu_1 < 0;$
- c)  $\mu \in L_1^+, \mu_2 < 0;$
- d)  $\mu \in L_2^+, \mu_2 < 0;$
- e)  $\mu \in L_2^\mp;$
- f)  $\mu \in L_1^\mp;$
- g)  $\mu \in L_1^-, \mu_1 > 0;$
- h)  $\mu \in L_2^-, \mu_1 > 0;$
- i)  $\mu \in L_2^+, \mu_2 > 0;$
- j)  $\mu \in L_1^+, \mu_2 > 0;$
- k)  $\mu \in L_1^\pm;$
- l)  $\mu \in L_2^\pm.$

# Comments on the attractors

---

1. Only the regions I,II,...,VI are related to non-chaotic dynamics (like the flow). The global attractors are **invariant curves**  $C^+$ ,  $C^-$  and/or  $C^*$ .
2. In the chaotic regions, the closure of the invariant manifolds can contain a **quasi-attractor**: a nontrivial attracting invariant set which contains stable p.o. (**sinks**) and/or **SA** (maybe made by several pieces). Arbitrarily small perturbations of the parameters when a SA is found can give rise to sinks.
3. There appear **strange attractors** of **different nature**:
  - $A^+$ ,  $A^-$  and  $A^*$  are born under the break-down of the closed invariant curves  $C^+$ ,  $C^-$  and  $C^*$ : Due to the **folding** of the curve it becomes **tangent to stable foliation** of the saddle fixed point.
  - The global attractors  $AT^+$ ,  $AT^-$  and  $GA$  are “homoclinic attractors” related to the intersection of (some or all) the invariant manifolds.
  - SA can also appear at the end of a **period doubling cascade** of sinks. These attractors have **local character**.

# Tail attractors

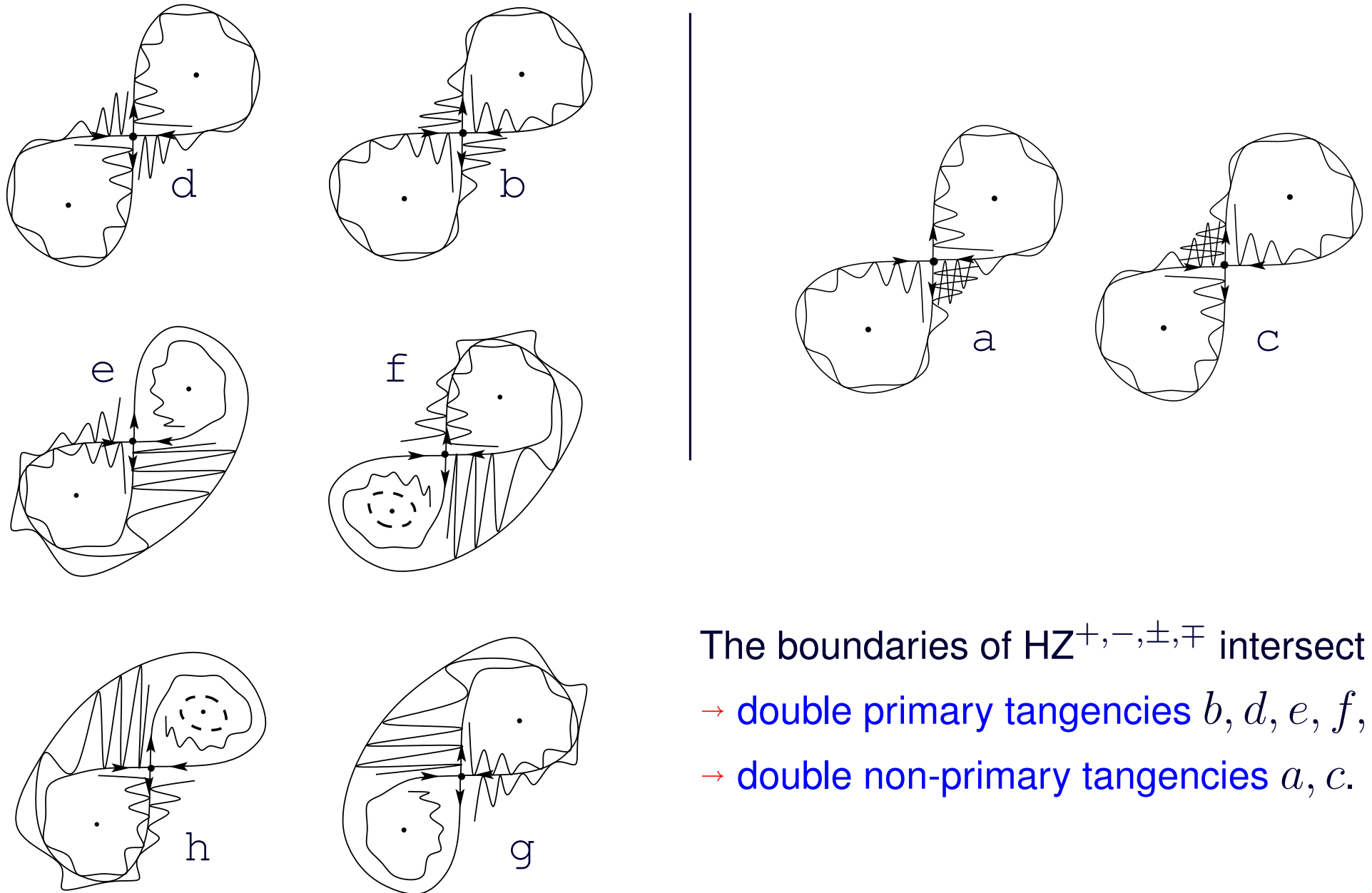


## Homoclinic intersections:

(a) “Tail” strange attractor  $AT^+$  ( $\mu \in 26$ )

(b) Global strange attractor  $GA$  ( $\mu \in 19$ )

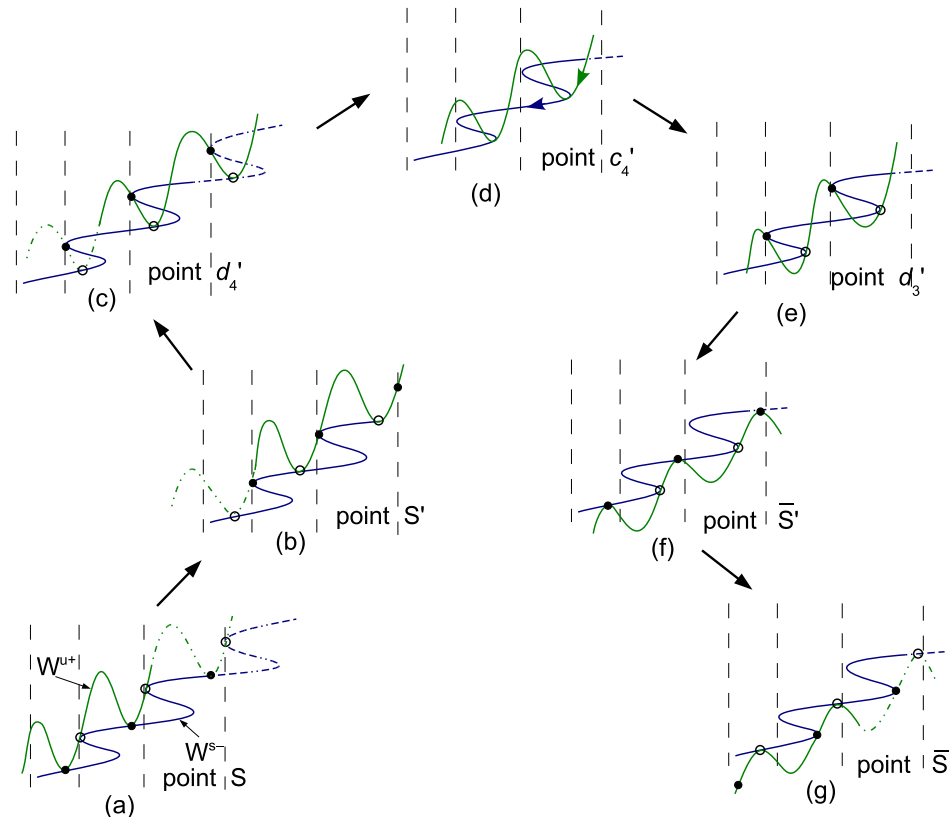
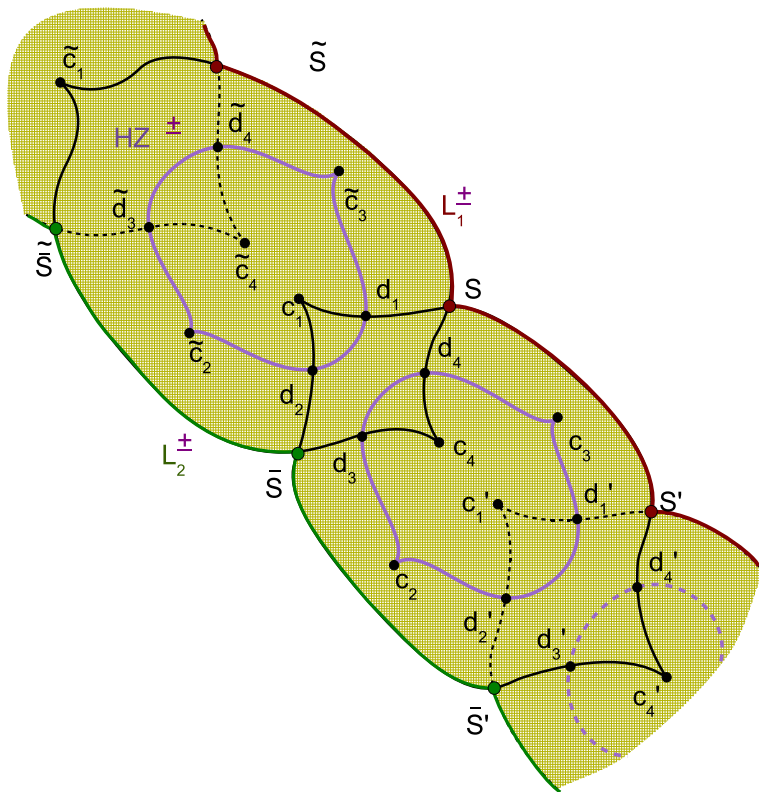
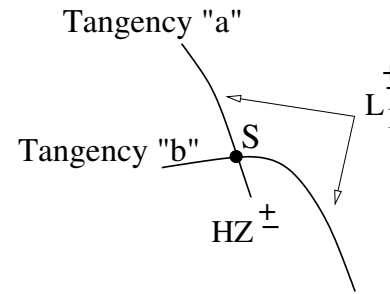
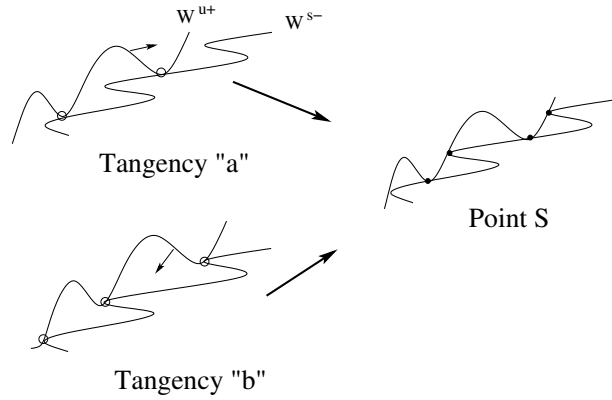
# Double homoclinic tangencies



The boundaries of  $HZ^{+, -, \pm, \mp}$  intersect at

- double primary tangencies  $b, d, e, f, g, h$
- double non-primary tangencies  $a, c$ .

# The stepness of $HZ^{\pm, \mp}$



**cubic tangencies!**



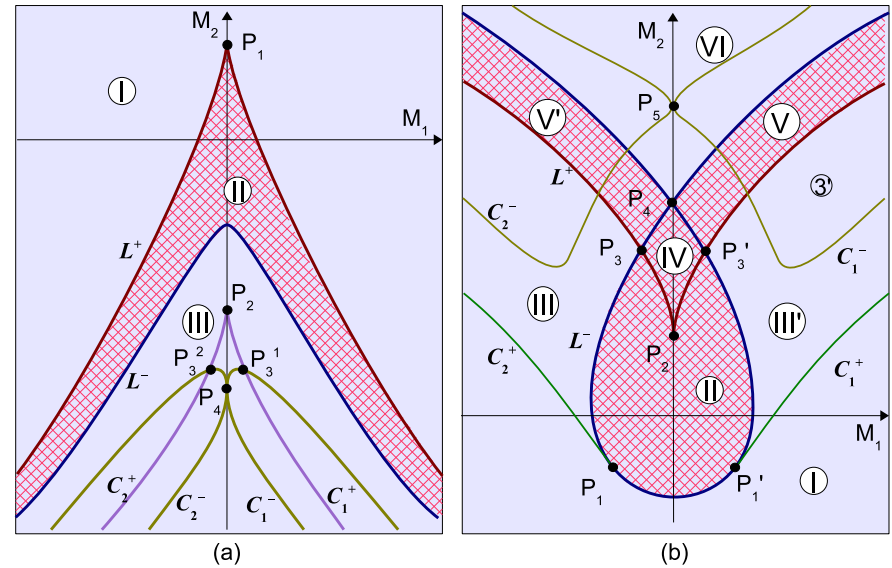
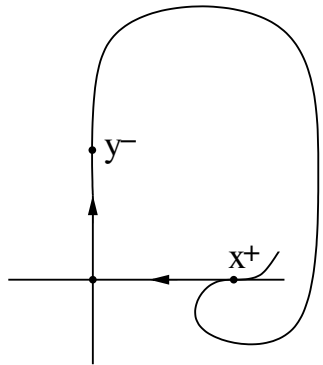
# Cubic single-round homoclinic tangencies

Outer map:

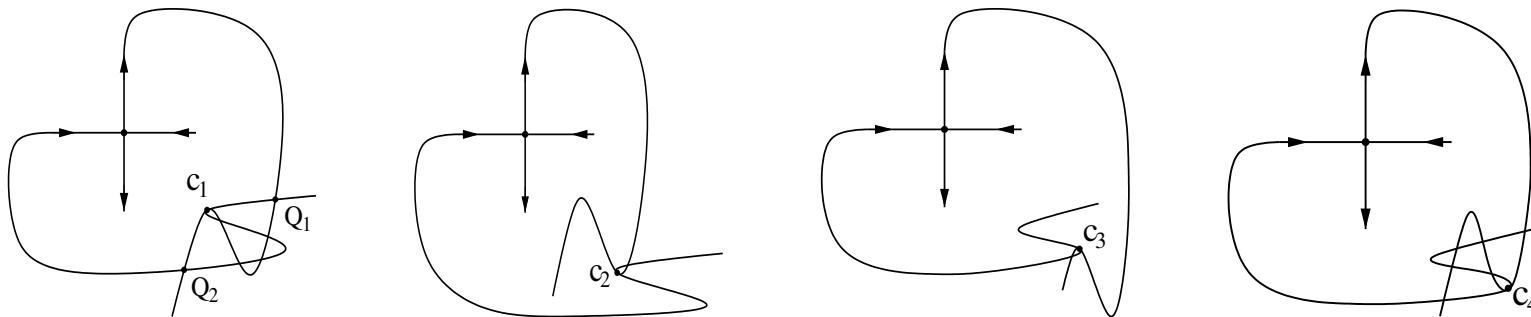
$$\begin{aligned}\bar{x} - x^+ &= ax + b(y - y^-), \\ \bar{y} &= cx + d(y - y^-)^3.\end{aligned}$$

Single round  $k$ -p.o,  $k$  large,  
**limit** return map:

$$\begin{aligned}\bar{X} &= Y, \\ \bar{Y} &= M_1 + M_2 Y + \text{sign}(d)Y^3.\end{aligned}$$

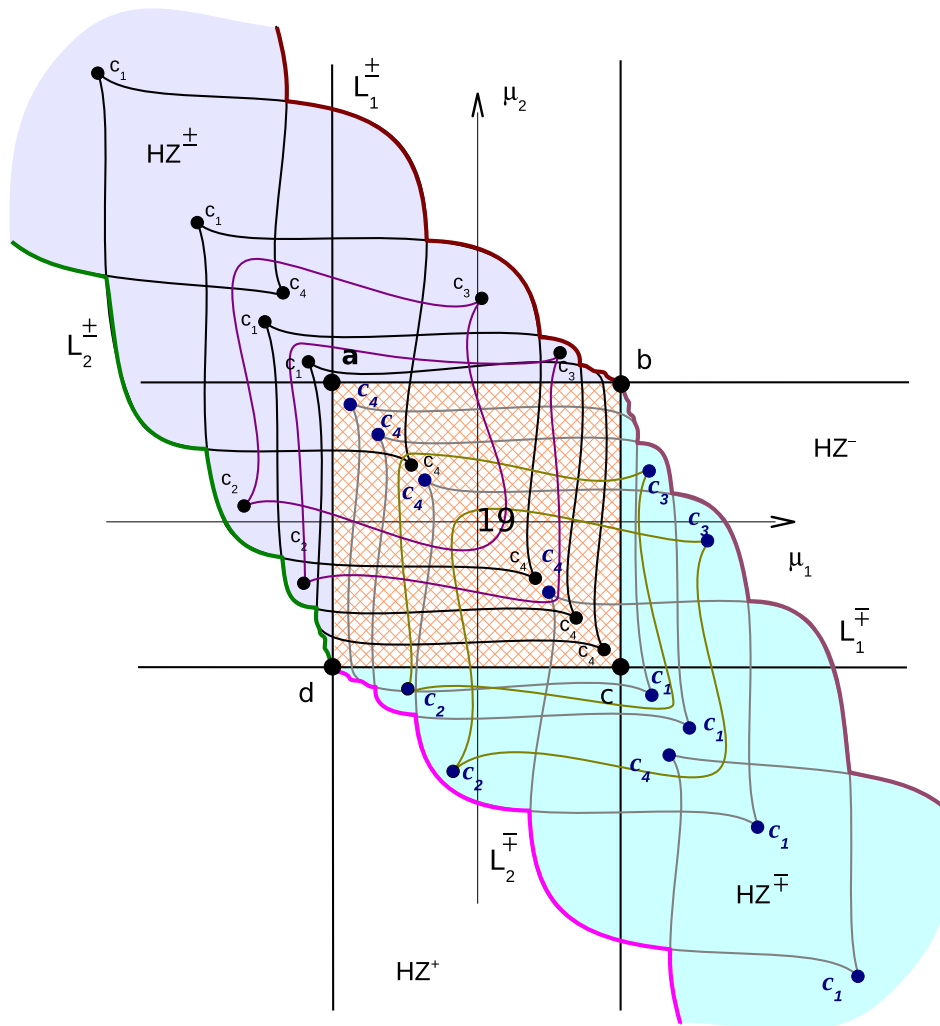


In our system,  $c_1, \dots, c_4$  cubic tangencies inside  $HZ^\pm$  and  $HZ^\mp$ .



**Lemma.** All the cubic tangencies  $c_1, \dots, c_4$  are of **spring-area type** ( $d < 0$ ).

# Accumulation of links inside $HZ^\pm$



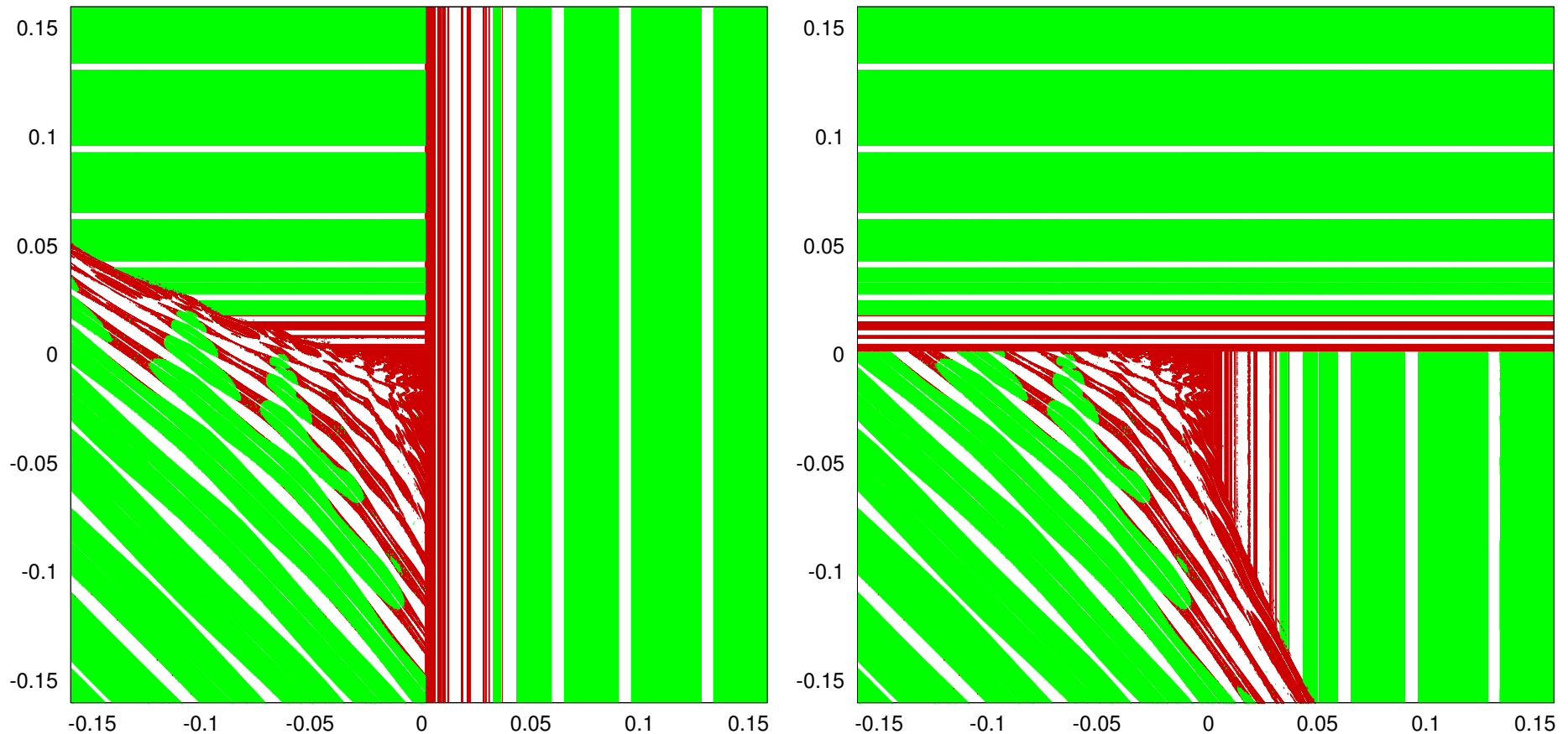
## Lemma.

1. The primary cubic tangencies  $c_1$  can exist only if  $W^{u+} \cap W^{s+} = \emptyset$  and  $W^{u-} \cap W^{s-} = \emptyset$  (i.e. in the regions **3** and **10** of the bif. diagram).
2. The primary cubic tangencies  $c_2$  can exist if  $W^{s+} \cap W^{u+} = \emptyset$  (i.e. in the regions **3**, **10** and **18**).
3. The primary cubic tangencies  $c_3$  can exist if  $W^{s-} \cap W^{u-} = \emptyset$  (i.e. in the regions **3**, **10** and **15**).
4. In the region **19** of the bif. diagram only primary cubic tangencies  $c_4$  can exist.

**Corollary.** The cusp points  $c_1, c_2, c_3$  and  $c_4$  accumulate to the points  $a, d, b$  and  $c$  resp.

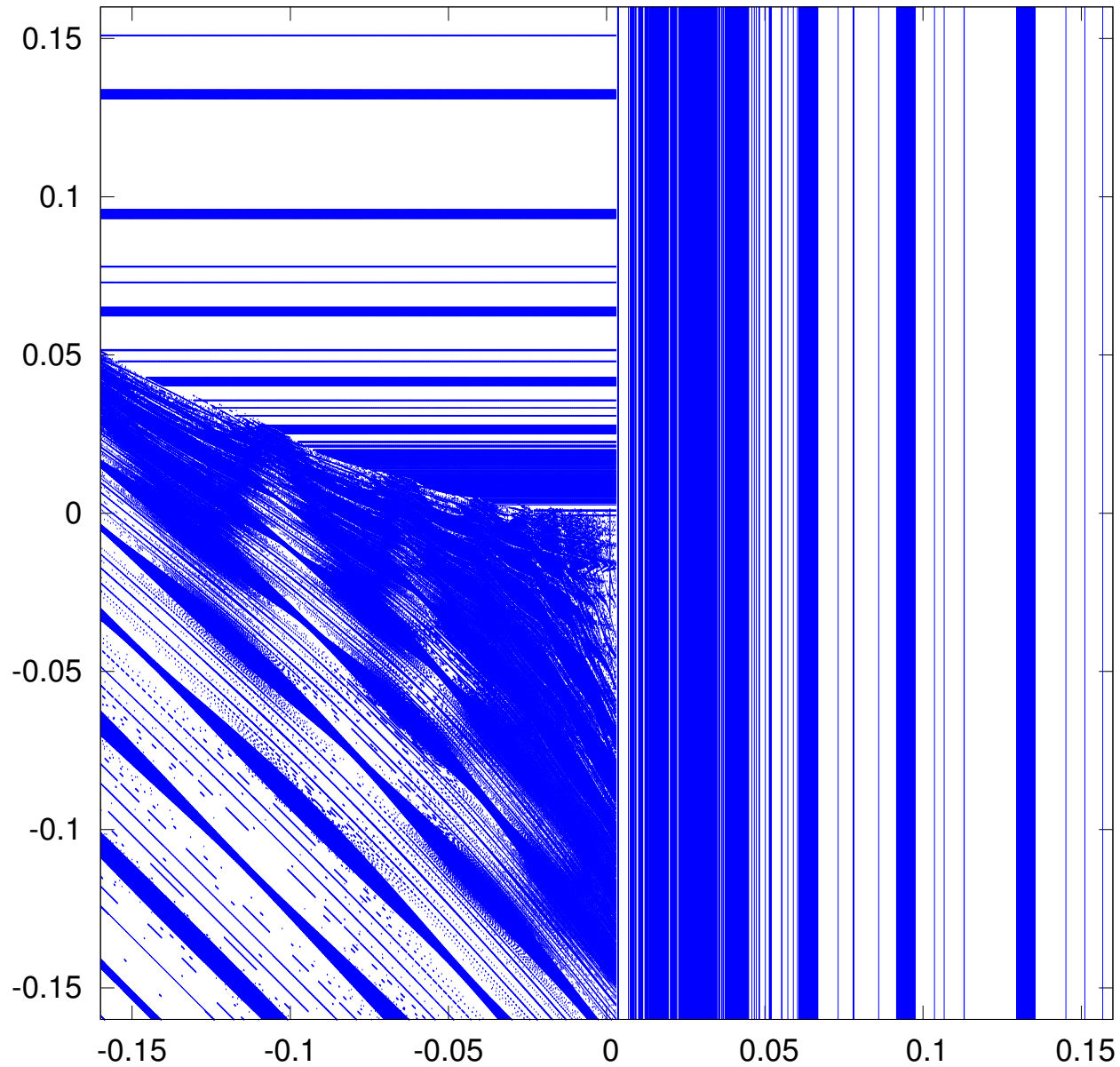
# Further analysis of the model: MLE

For each  $(a_1, a_2)$ -parameters we take  $z_0 = 0.5$ ,  $\eta_0 = 0$  and  $s_0 = 1$  (left) or  $s_0 = 1$  (right) as i.c. (i.e. on  $W^u$ ) and compute the Max. Lyap. exp.  $\Lambda$ .

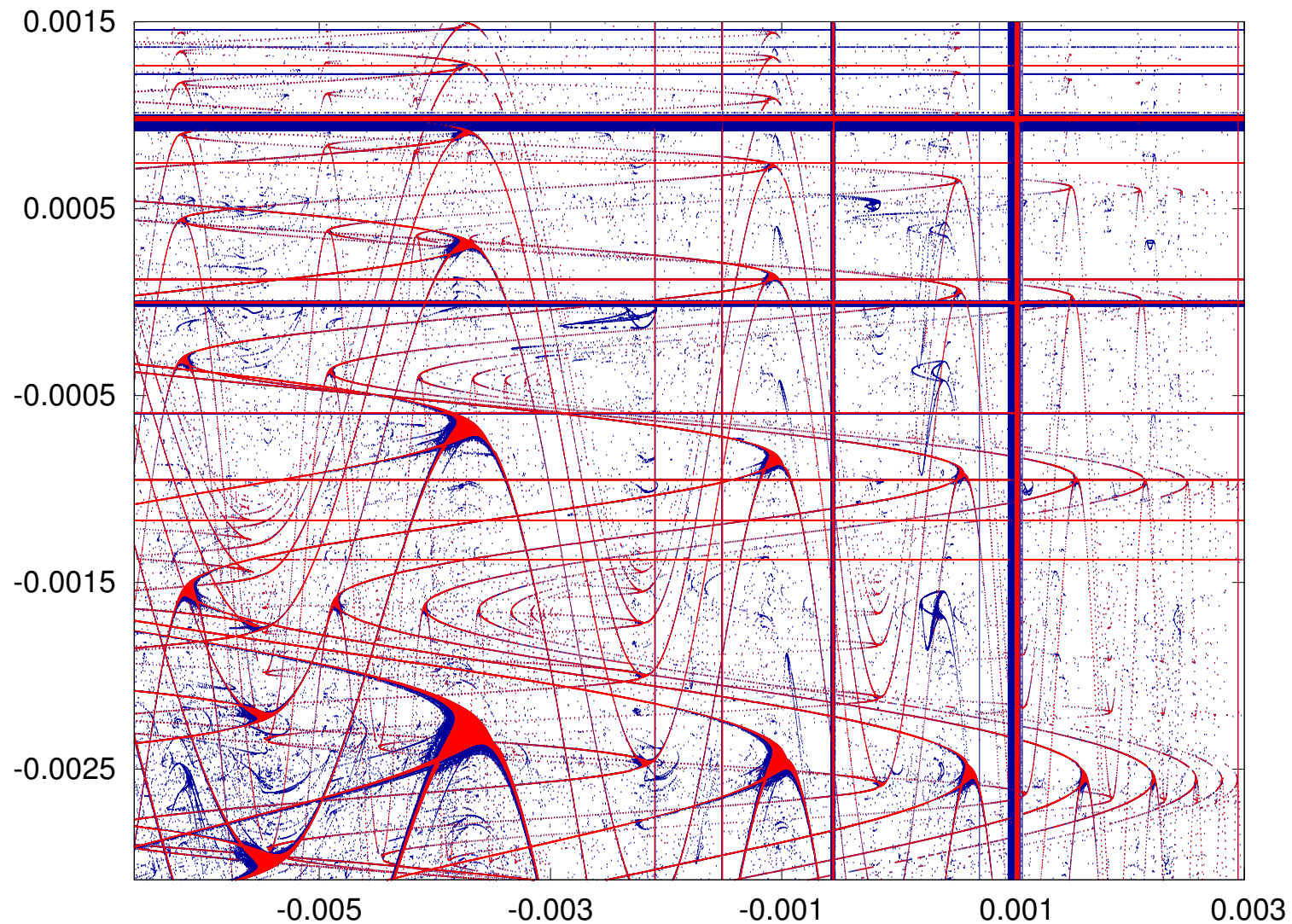


**Red** points correspond to  $\Lambda > 0$  (**chaotic attractor**), **green** points to  $\Lambda = 0$  (**invariant curve**) and **white** points to  $\Lambda < 0$  (**periodic sink**).

# Stability regions ( $\Lambda < 0$ ) related to periodic sinks



# Stability region: magnification

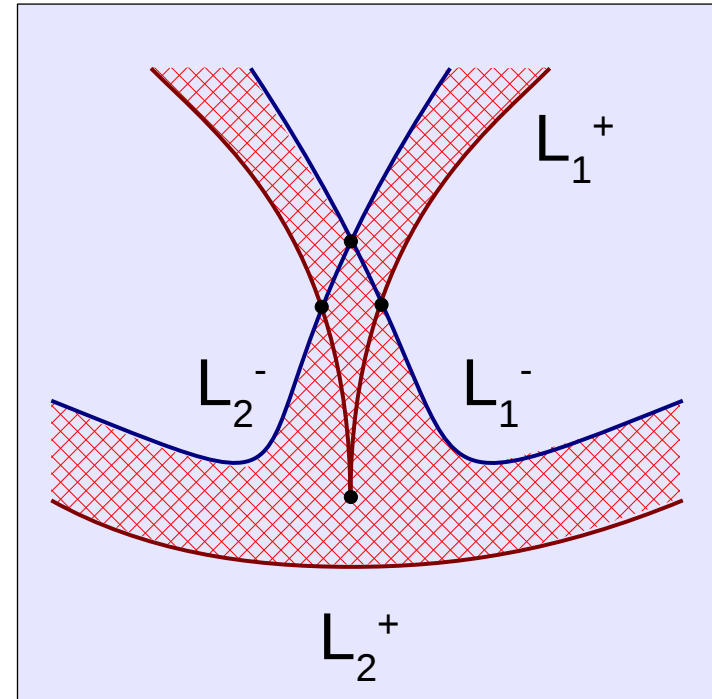


**Blue:** set of  $(a_1, a_2)$ -parameters with  $\Lambda < 0$  for the i.c.  $(0.5, 0, 1)$ . The attractor is a **periodic sink**.

**Red:** parameters for which there is a **2-periodic sink** as attractor.

# The cross-road scenario

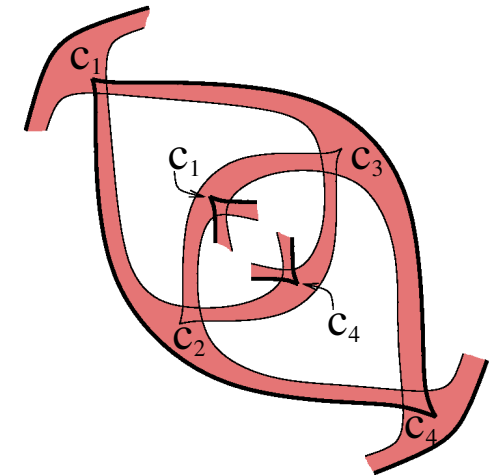
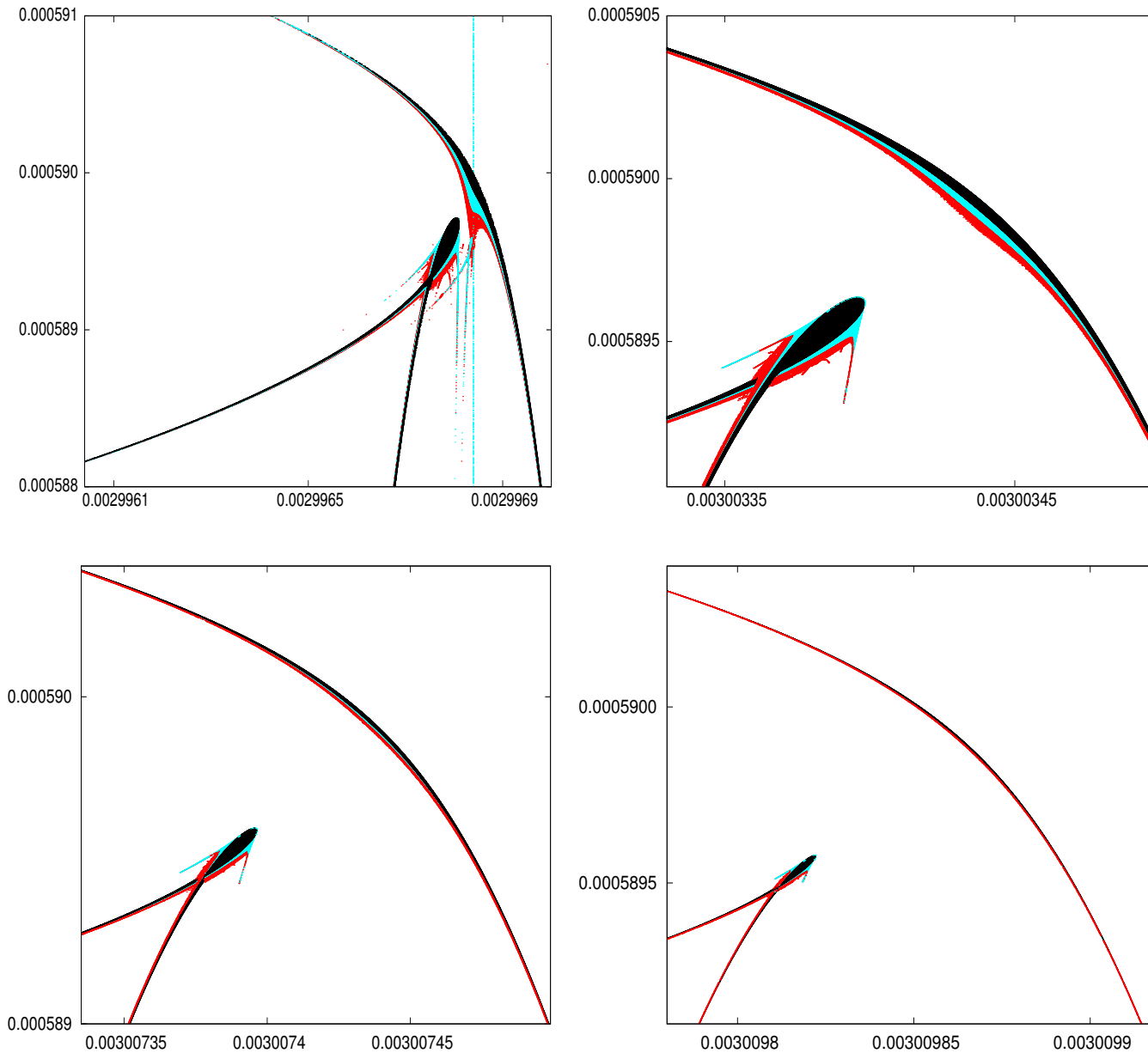
If  $k$  is **not large enough** (depending on the parameters) other configurations might appear (non-local effects and role of high order terms in the return map). One of this, which is commonly observed in numerical explorations and related to the spring-area configuration, is the **cross-road scenario**.



H. Broer, C. Simó and J.C. Tatjer. *Towards global models near homoclinic tangencies of dissipative diffeomorphisms*. Nonlinearity, 1998, 11, 667–770.

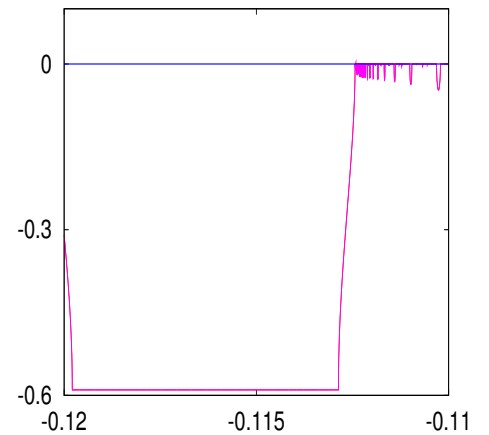
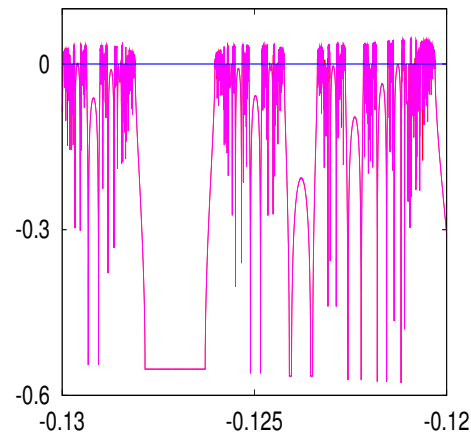
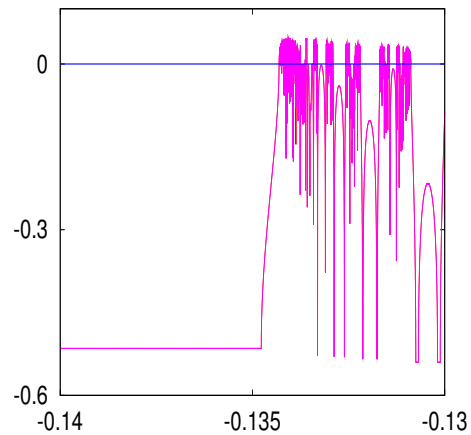
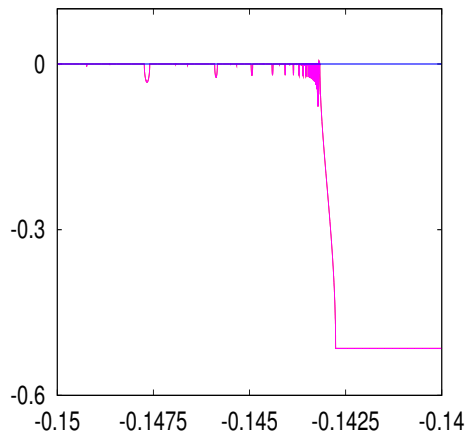
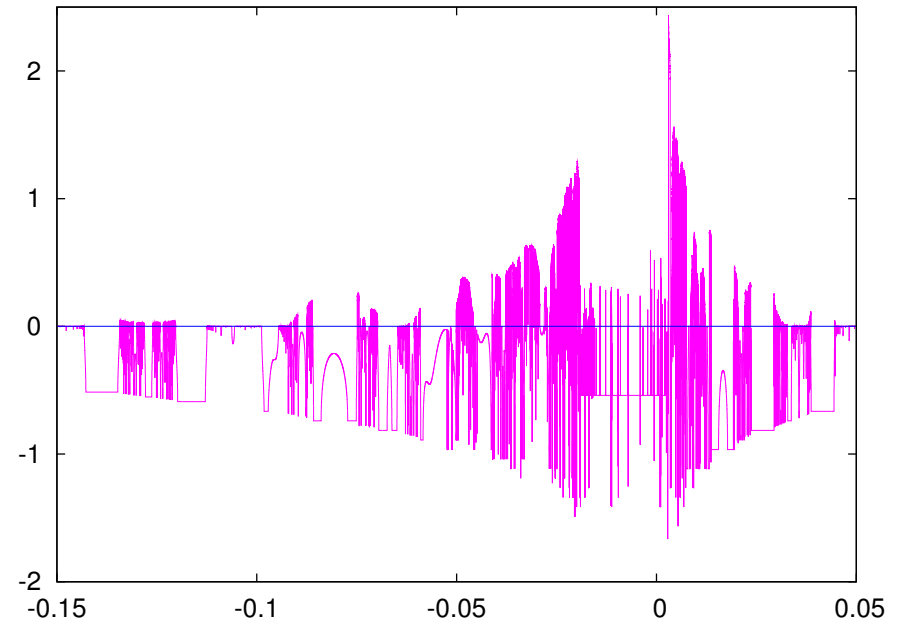
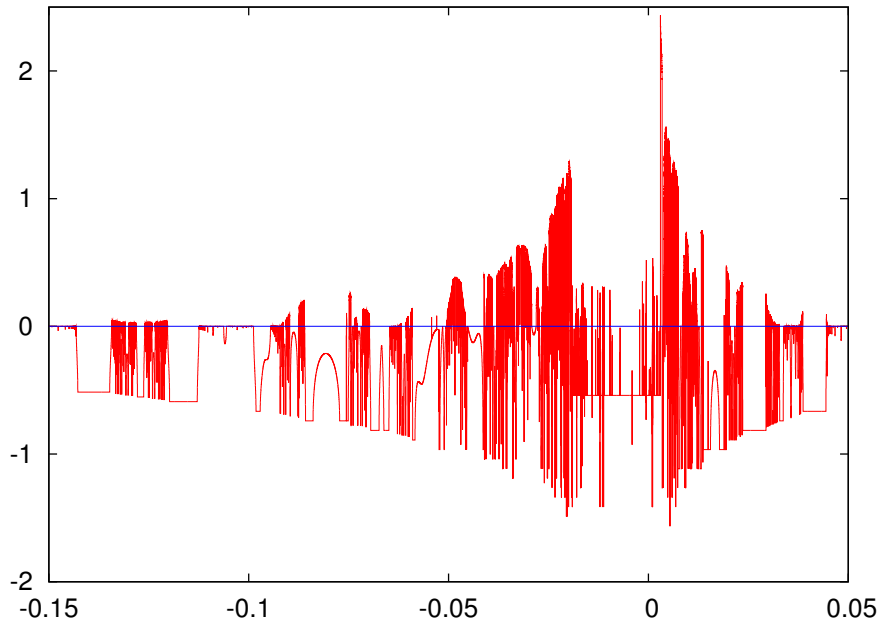
J.P. Carcassès, C. Mira, M. Bosch, C. Simó and J.C. Tatjer. “Crossroad area-spring area” transition (I)-(II). *Parameter plane representation*. Int. J. Bifur. and Chaos, 1991, 1.

# Transition to spring-area: larger (return) periods



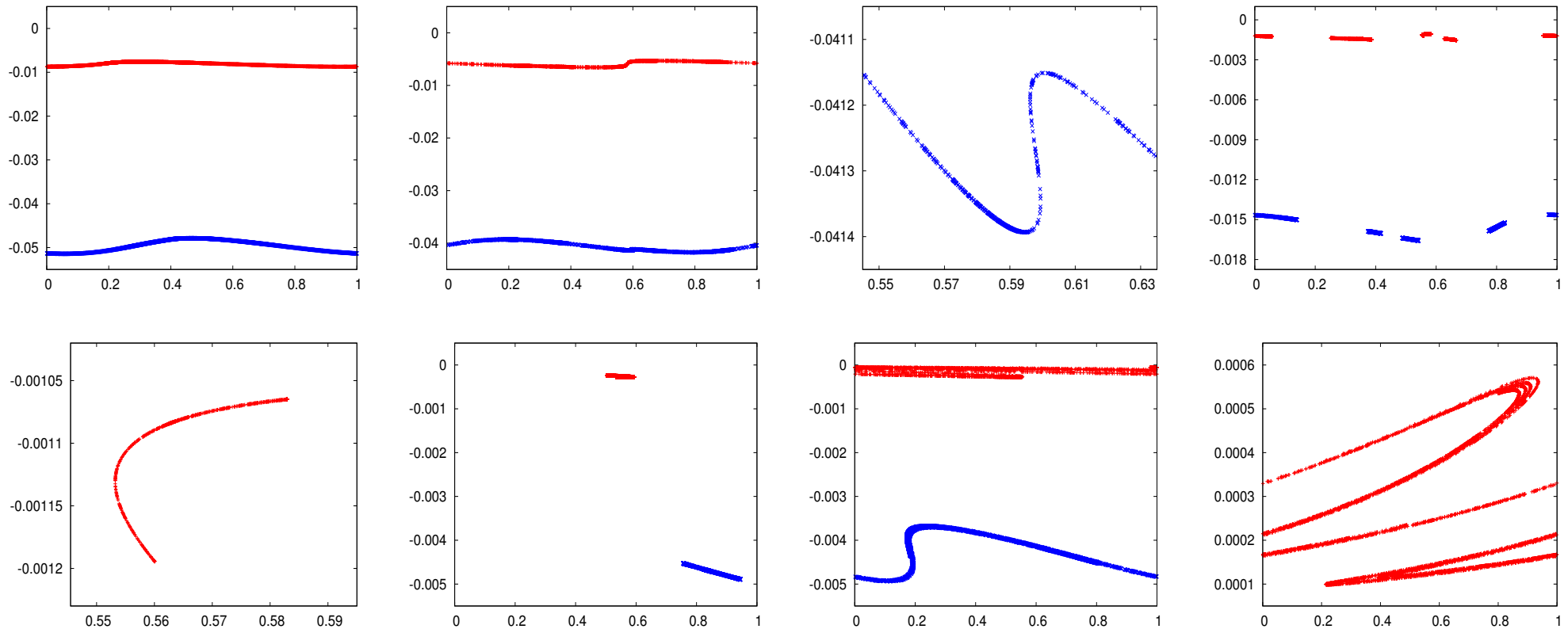
Note the progressive destruction of the previous cross-road domain.

# Lyapunov exponents



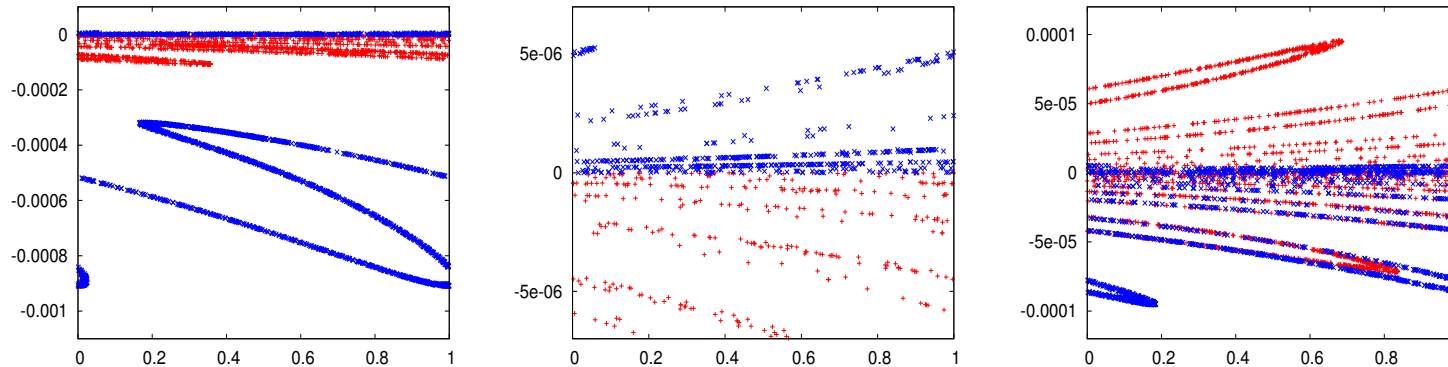


# A sample of attractors I ( $a_2 = 0$ )



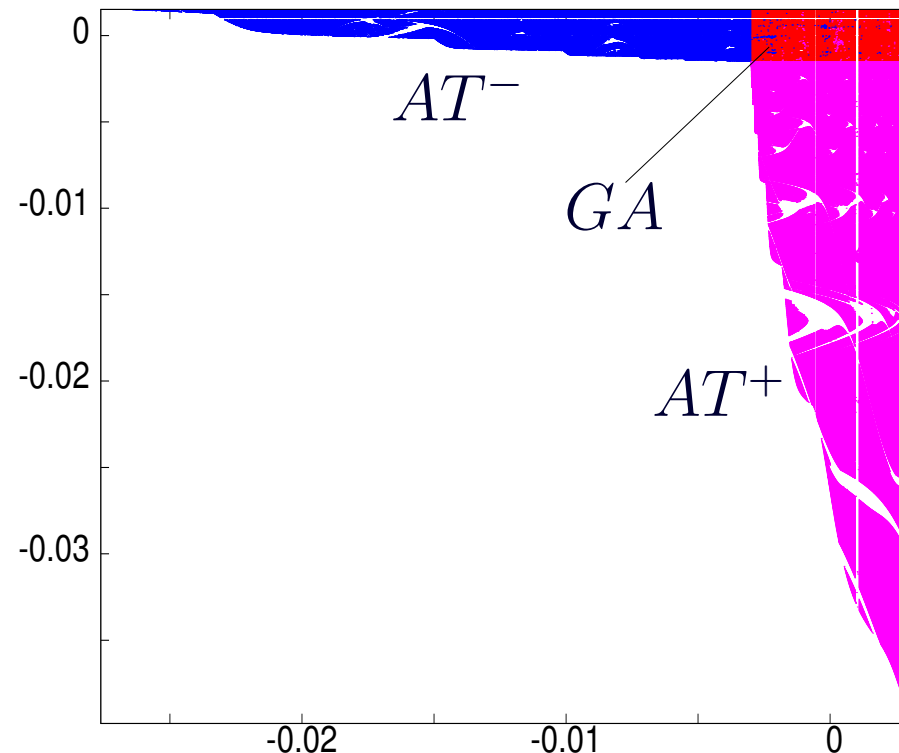
**1st row:** invariant curve ( $a_1 = -0.145$ ), SA of type  $A^*$  with a global nature ( $a_1 = -0.129$ ), detail of the fold in the previous SA ( $a_1 = -0.129$ ) and a SA of type  $A^*$  with a local periodic nature ( $a_1 = -0.073$ ). **2nd row:** Detail of the Hénon-like structure of the previous SA ( $a_1 = -0.073$ ), SA of type  $A^*$  with a local nature ( $a_1 = -0.034$ ), globalization of the previous SA ( $a_1 = -0.033$ ) and a SA of type  $A^-$  ( $a_1 = 0.006$ ).

# A sample of attractors II ( $a_2 = -0.001$ )



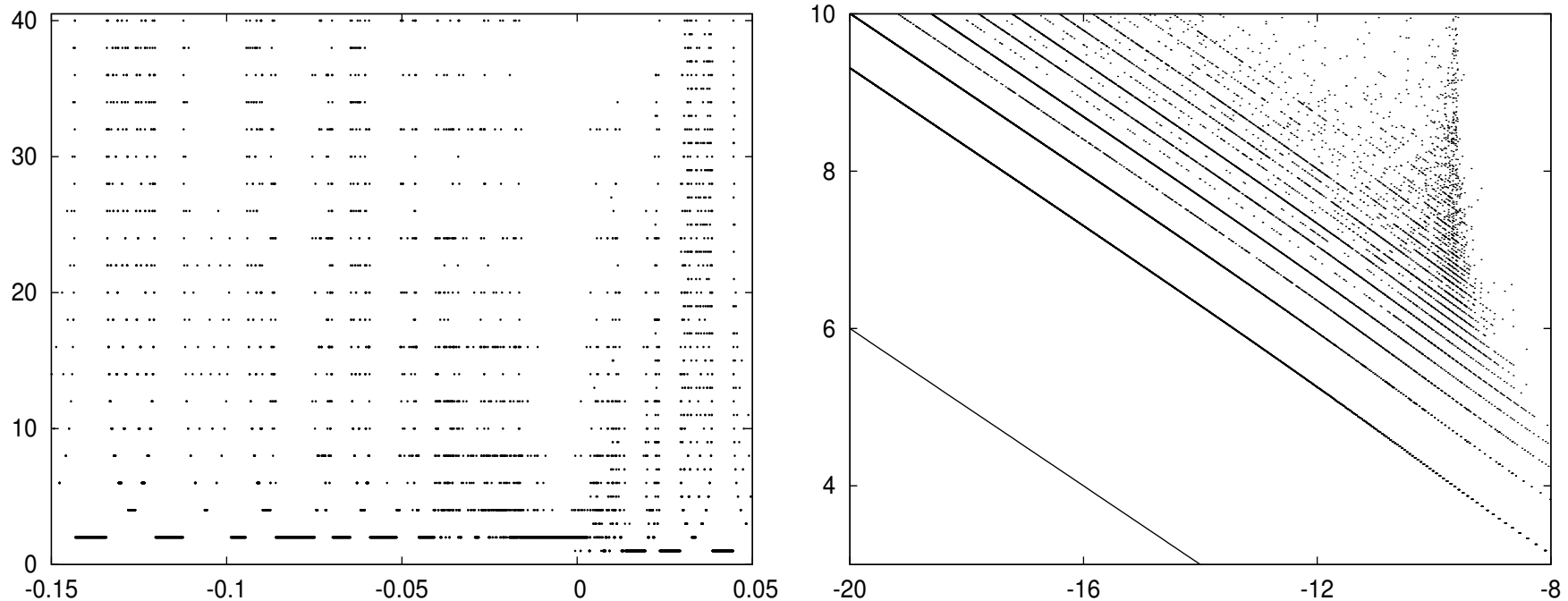
Left: Tail attractor of type  $AT^-$  ( $a_1 = -0.0095$ ). Center: Magnification of the previous figure. Right: Global SA of type  $GA$  ( $a_1 = 0$ ).

We can identify the points  $e$  and  $g$  of the bif. diagram. The white domains contained in these colored regions correspond to sinks.



# The period of the sinks

**Lemma.** If a s-n appears for a critical value  $a_1 = a_{1,c}$ , then the period of nearby sinks behaves as  $\text{ctant} \times |a_1 - a_{1,c}|^{-1/2}$ .



$a_2 = 0$ . We plot Per vs.  $a_1$  (left) and  $\log(\text{Per})$  vs  $\log(a_1 - a_{1,c})$  (right).

$a_{1,c} \approx -0.143170413565918$  is the value for the first appearance of period 2 orbits with  $a_1 > -0.15$ .

All periods (under  $M$ ) from 24 to 11026 have been detected!

# Open problems and extensions

---

Several questions remain **open**, like

- The **creation/destruction** of SA by **folding** of IC. In particular the **boundary marked as BD** in the bifurcation diagram.
- The **abundance** of sinks, taking into account the existence of **cross-road and spring** areas.
- **Links with s-n boundaries** connecting different cross-road and spring areas.
- Relative **size** of the **basins of attraction** when there is **multiplicity of attractors**.

... and possible **extensions** to **3D and higher dimension** diffeomorphisms.

E.g.: Shilnikov-like, Hopf-Shilnikov-like maps, etc.



**Thanks for your attention!!**